Induction of Supramolecular Chirality in the Self-Assemblies of Lipophilic Pyrimidine Derivatives by Choice of the Amino Acid-Based Chiral Spacer

ARTICLE *in* CHEMISTRY - A EUROPEAN JOURNAL · AUGUST 2013

Impact Factor: 5.73 · DOI: 10.1002/chem.201300605 · Source: PubMed

3 AUTHORS:

Sougata Datta
Indian Institute of Science
15 PUBLICATIONS **135** CITATIONS
SEE PROFILE

Suman Kalyan Samanta
Bergische Universität Wuppertal
23 PUBLICATIONS **493** CITATIONS
SEE PROFILE

Santanu Bhattacharya
Indian Institute of Science
236 PUBLICATIONS **6,475** CITATIONS
SEE PROFILE

CHEMISTRY
A EUROPEAN JOURNAL

ChemPubSoc
Europe

DOI: 10.1002/chem.201300605

Induction of Supramolecular Chirality in the Self-Assemblies of Lipophilic Pyrimidine Derivatives by Choice of the Amino Acid-Based Chiral Spacer

Sougata Datta,[a] Suman K. Samanta,[a] and Santanu Bhattacharya*[a, b]

Abstract: A new family of supramolecular organogelators, based on chiral amino acid derivatives of 2,4,6-trichloro-pyrimidine-5-carbaldehyde, has been synthesized. L-alanine was incorporated as a spacer between the pyrimidine core and long hydrocarbon tails to compare the effect of chirality and hydrogen bonding to that of the achiral analogue. The role of aromatic moiety on the chiral spacer was also investigated by introducing L-phenyl alanine moieties. The presence of intermolecular hydrogen-bonding leading to the chiral self-assembly was probed by concentration-dependent FTIR and UV/Vis spectroscopies, in addition to circular dichroism (CD) studies. Temperature and concentration-dependent CD spectroscopy ascribed to the formation of β-sheet-type H-bonded networks. The morphology and the arrangements of the molecules in the freeze-dried gels were examined by scanning electron microscopy (SEM), transmission electron microscopy (TEM), atomic force microscopy (AFM), and X-ray diffraction (XRD) techniques. Calculation of the length of each molecular system by energy minimization in its extended conformation and comparison with the small-angle XRD pattern reveals that this class of gelator molecules adopts a lamellar organization. Polarized optical microscopy (POM) and differential scanning calorimetry (DSC) indicate that the solid state phase behavior of these molecules is totally dependent on the choice of their amino acid spacers. Structure-induced aggregation properties based on the H-bonding motifs and the packing of the molecule in three dimensions leading to gelation was elucidated by rheological studies. However, viscoelasticity was shown to depend only marginally on the H-bonding interactions; rather it depends on the packing of the gelators to a greater extent.

Keywords: amino acid · cotton effect · helical nanofiber · hydrogen bonding · self-assembly · viscoelasticity

Introduction

The spontaneous formation of self-assembly is a remarkable phenomenon in nature that helps in the transcription of interesting features from molecular level to complex supramolecular structures through specific molecular interactions.[1] In this context, low molecular-weight organogelators (LMOGs)[2] have received remarkable interest because of the reliable formation of various self-assembled three-dimensional superstructures. They have proven to be attractive candidates for diverse range of applications in a number of different fields, including the design and synthesis of nanomaterials,[3] biomaterials,[4] sensors,[5] stimuli-responsive materials,[6] and in molecular electronics,[7] and catalysis.[8] Self-assembly, which underpins a nanoscale structure, reflects the individual components and the supramolecular ordering as a result of multiple non-covalent interactions (i.e., H-bonding, π–π stacking, solvophobic effects, van der Waals forces, charge-transfer interactions, metal–ligand coordination, etc.). For example, the main driving force among amides,[9] urethanes,[10] ureas,[11] and sugar derivatives[12] is hydrogen bonding, with van der Waals forces dominant[13] among steroid derivatives. Some gelators utilize two or more of these interactions.[14] The reversible systems may be potentially applied to drug-delivery systems[15] and supramolecular "switch" systems with appropriate memory functions.[16] Self-assemblies of the LMOGs are inherently responsive toward thermal stimulus and show reversible sol-to-gel transitions when their heated solutions are cooled below the respective gelation temperatures.[17]

Naturally occurring pure chiral amino acid-based LMOGs have received special attention because of their potential applications in the pharmaceutical industry as soft materials for drug-delivery and tissue engineering. Amino acid- or peptide-based hydrogelators have gained importance because of the biocompatibility of the constituent materials (amino acids).[18] We have previously reported that the organogelators of fatty acid amides of L-alanine can gelate oil selectively from oil–water mixtures.[19] Since then, several reports have appeared in the literature addressing this important problem of phase-selective gelation.[20,21]

[a] S. Datta, Dr. S. K. Samanta, Prof. Dr. S. Bhattacharya
Department of Organic Chemistry, Indian Institute of Science
Bangalore 560 012, Karnataka (India)
Fax: (+91) 80-2360-0529
E-mail: sb@orgchem.iisc.ernet.in

[b] Prof. Dr. S. Bhattacharya
Jawaharlal Nehru Centre for Advanced Scientific Research
Bangalore 560 064, Jakkur (India)

Supporting information for this article is available on the WWW under http://dx.doi.org/10.1002/chem.201300605.

Attaching one amino acid moiety through amide coupling creates H-bonding donor (N–H) and -acceptor (C=O) sites in the resulting molecule. This enhances their propensity to self-assemble in solution to produce various types of supramolecular structures (helices, β-sheets, fibers, nanosheets, nanotapes, nanotubes, etc.), a number of which lead to gel formation.[21,22] The fibers inside such gel networks could template different kinds of nanomaterials to give rise to new nanocomposites with interesting properties.[3] In this respect, the role of the solvent in which the gelator forms the self-assembled structures is also crucial; the solvent–gelator interactions play a great role to produce different morphologies.[23]

Recently, Fenniri and co-workers have introduced an excellent molecular template based on 4-chloro-2,6-bis(octadecylamino) pyrimidine-5-carbaldehyde, which self-assembles into a fibrous lamellar structure in both the dry solid and the gel state.[17c] However, the self-assemblies of 2,4,6-trichloro-pyrimidine-5-carbaldehyde derivatives containing two dissimilar residues are still unknown. It occurred to us that grafting such molecular templates with natural chiral amino acids might produce interesting supramolecular organizations. Here, we investigate the corresponding chiral self-assemblies in solution by circular dichroism (CD) spectroscopy. These studies offer an opportunity to acquire valuable information about the nature of packing in the molecular level and provide new ways of designing useful soft materials.

Herein, we introduce a family of organogelators based on L-amino acid derivative of 2,4,6-trichloro-pyrimidine-5-carbaldehyde. We took the advantage of this molecule, which allows incorporation of more than one amino moiety by successive substitution of the chloride groups by different amines.[24] L-Alanine has been selected for the incorporation as one of the simplest chiral counterparts. Further substitution with L-phenylalanine introduces an element of inter-aromatic interactions. Also, the number of the amino acid moieties has been varied to see the effect this has on the self-assembly in solution. Thus, the incumbent chiral phenomenon could be compared with the corresponding achiral analogue. The gelation property of these compounds was examined in hydrocarbons such as, *n*-hexane, *n*-heptane, and *n*-dodecane. The thermal and mechanical properties were investigated in the solid and gel phase, respectively, to find out the role of H-bonding through the L-amino acid-based spacer on the self-assembly process.

Results and Discussion

A series of organogelators were synthesized based on 2,4,6-trichloro-pyrimidine-5-carbaldehyde as the building block and chiral amino acid moieties were inserted in the side chains by using amide bond formation. Compared with the simple achiral analogue **5** (Figure 1), we have introduced an L-alanine spacer as the simplest chiral moiety (**1** and **3**) and further extended this to L-phenylalanine (**2** and **4**) to understand the effect of π–π interaction in the self-aggregation process. The gelators were synthesized by using chlorination of barbituric acid followed by nucleophilic attack with corresponding amines to obtain the final gelators in moderate to high yields (see Scheme S1 in the Supporting Information). Each new compound and the intermediates were characterized by ^{1}H and ^{13}C NMR spectroscopy, ESI-MS, matrix-assisted laser desorption/ionization mass spectrometry (MALDI MS), FTIR, and elemental analysis (see the Experimental Section in the Supporting Information).

In the following sections, we report the physical characterization of different modes of aggregation and gelation properties of the compounds shown in Figure 1, in a number of aromatic and aliphatic hydrocarbons and investigate the role of the amino acid-based chiral spacer on the self-assembly process.

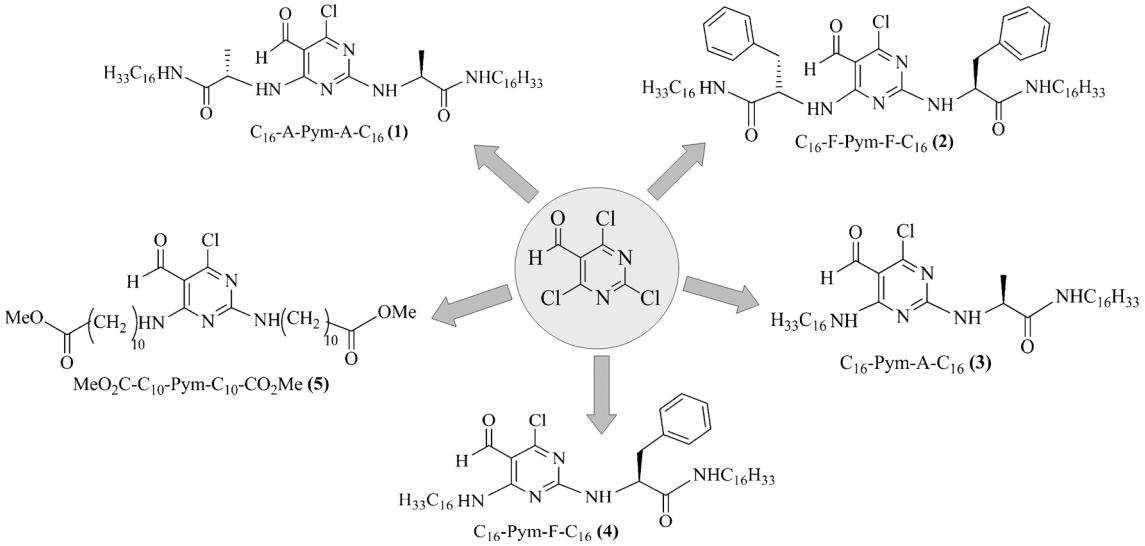

Figure 1. Molecular structures of various amino acid based gelators derived from 2,4,6-trichloropyrimidine-5-carbaldehyde.

Gelation studies: The gelation of each of these compounds (**1**–**5**) was tested in different aromatic hydrocarbons, lower molecular weight aliphatic alcohols, and aliphatic hydrocarbons. Their attempted gelation in toluene, CH_2Cl_2, $CHCl_3$, and THF led to sol formation in every instance. However, they were found to be insoluble in polar aliphatic alcohols, for example, ethanol and *n*-butanol, due to a polarity mismatch. Achiral compound **5**, having no amino acid moiety, formed an opaque gel only in aliphatic hydrocarbons and failed to gelate aromatic hydrocarbons. Hydrolysis of gelator **5** produced the di-acid derivative (COOH-C_{10}-Pym-C_{10}-COOH), which remained insoluble in each of the hydrocarbon and aromatic solvents undertaken for gelation study, perhaps due to the high polarity of the di-acid. However, other members formed clear, transparent gels in hydrocarbons (Figure 2). Also, increasing the chain length of the aliphatic hydrocarbons from *n*-heptane to *n*-dodecane, the

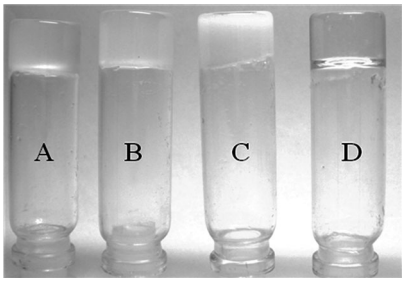

Figure 2. Photograph showing organogels of **1** (A), **3** (B), **5** (C), and **4** (D) in *n*-dodecane.

minimum gel concentration (mgc) value of each of these gelators decreased indicating better van der Waals interactions between the aliphatic chains of the gelators and the solvent (Table 1). It was observed that compound **3**, which was decorated with one L-alanine-based spacer, formed most efficient transparent gel in *n*-dodecane and the mgc value (2 mM) of **3** was found to be the lowest among all the members in this family of gelators. However, the di-substituted derivative **1** showed higher mgc compared with that of the monosubstituted compound **3**. Interestingly, compounds **1** and **3** did not show any difference in their mgc values (2.8 mM) in *n*-heptane probably because van der Waals interactions between the aliphatic chains of the gelators and the solvent is less prominent in *n*-hexane relative to that in *n*-dodecane. Moreover, compound **4** with one L-phenylalanine moiety was capable of immobilizing aliphatic hydrocarbons. In contrast, compound **2**, containing two L-phenylalanine spacers, resulted in sol formation in both aliphatic and aromatic hydrocarbons. This suggests that the, presence of aromatic ring may allow a π–π stacking interaction among them but an excess of which may disfavor the intermolecular aggregation process necessary for gelation.

Table 1. Gelation ability of compounds **1**–**5** in different solvents.[a]

Compound	Toluene	*n*-Heptane	*n*-Dodecane
C_{16}-A-Pym-A-C_{16} (**1**)	S	TG (2.8)	TG (2.8)
C_{16}-F-Pym-F-C_{16} (**2**)	S	S	S
C_{16}-Pym-A-C_{16} (**3**)	S	TG (2.8)	TG (2)
C_{16}-Pym-F-C_{16} (**4**)	S	TG (8)	TG (7.8)
MeO_2C-C_{10}-Pym-C_{10}-CO_2Me (**5**)	S	OG (12.6)	OG (8.7)

[a] OG = opaque gel, TG = transparent gel; S = soluble. Parentheses contain the mgc (in mM) of the gelator molecules.

UV/Vis and circular dichroism (CD) spectroscopy: To obtain further insights into the intermolecular interaction in the supramolecular aggregates, concentration- and temperature-dependent UV/Vis spectra were recorded in *n*-dodecane. The concentration-dependent UV/Vis spectra of **1** in *n*-dodecane show a broad absorption in the range 250–350 nm and a sharp peak near 220 nm at higher concentrations (> 0.2 mM). When the concentration was decreased to 0.05 mM, two new bands near 265 and 310 nm appeared with the existing band at 220 nm (Figure 3a). The UV absorption peak observed near 220 nm may be attributed to the n–π* transition of the −CONH group, C=N, and C=C bonds. The UV absorption peaks at 265 and 310 nm most likely originated from the π–π* of the aromatic ring and n–π*transition of the formyl substituent, respectively.[25] The intensity of these

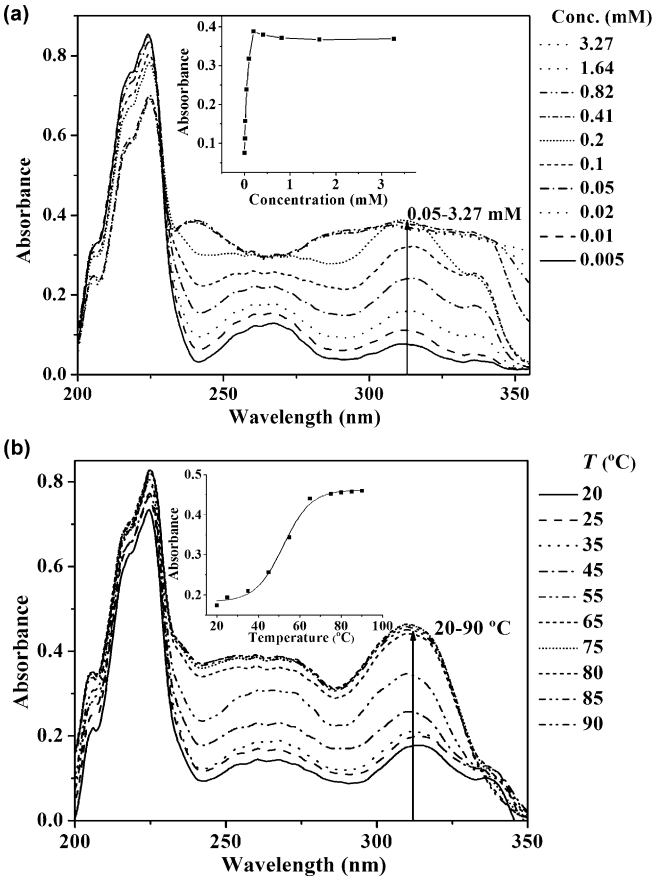

Figure 3. a) Concentration-dependent changes in the UV/Visible spectra of **1** in *n*-dodecane at 25 °C; inset shows the plot of absorbance versus concentration at 310 nm. b) Temperature-dependent changes in the UV/Vis spectra of **1** in *n*-dodecane at the concentration of 0.03 mM; inset shows the plot of absorbance versus temperature at 310 nm.

bands decreased steadily on further dilution (inset, Figure 3a).

It is evident from the concentration-dependent UV/Vis spectra of **1** in *n*-dodecane that the peaks are broadened at higher concentrations. Therefore, we recorded its temperature-dependent UV/Vis spectra at a lower concentration (0.03 mM). The peak intensities at 220, 265, and 310 nm increased monotonically with the increase of temperature and became saturated at approximately 75 °C (Figure 3b). This was a consequence of the weakening of the non-covalent interactions between the chromophores. This resulted in the breaking of the larger aggregates to form aggregates of shorter length.[17a] The thermotropic transition temperature (ca. 53 °C) of the aggregated species of **1** in UV/Vis spectroscopy was calculated by plotting peak intensity at 310 nm versus temperature (inset, Figure 3b). Other members in this family of gelators followed similar pattern in their concentration- and temperature-dependent UV/Vis spectra (see Figures S1 and S2 in the Supporting Information).

The self-assemblies of the gelator were investigated by using CD spectroscopy to understand the role of chirality of the individual molecules due to the presence of the chiral amino acid moieties. CD spectra as a function of concentration and temperature were recorded to unveil the mechanism and growth of the self-assembly process. As the gelator **1** showed aggregation-dependent CD signals, it was subjected to concentration variation in *n*-dodecane to probe its concentration effect at 25 °C. The CD spectra of **1** showed an intense negative band near 220 nm, ascribed to the n–π* transition of the −CONH group (Figure 4a). This signature is similar to the CD signature of peptides adopting the β-sheet secondary structure.[26] This observation indicates that extensive hydrogen-bonding is playing an important role to build up this supramolecular assembly of **1**. The characteristic CD signal at 220 nm was always observed during the concentration variation. The most notable phenomenon was observed near 328 nm. Only one negative peak at 220 nm was observed at a high concentration of **1** (3.27 mM) in *n*-dodecane (Figure 4a). When the concentration was decreased to 0.41 mM, the solution exhibited a new positive Cotton effect at 304 nm and a new negative Cotton effect near 328 nm with the existing negative band at 220 nm, indicating an anti-clockwise orientation of dipole moments in the supramolecular aggregates.[12b] This molecular helical arrangement of **1** was reflected in the mesoscopic left-handed helicity observable under the AFM study (discussed later). A further decrease in the gelator concentration up to 0.1 mM intensified these new peak intensities. At the concentration of 0.1 mM, the peak at 328 nm shifted to 326 nm along with broadening of the peak observed at 220 nm. However, the peak at 304 nm did not show a significant shift during the concentration variation. Interestingly, the intensity of the peaks at 304 and 326 nm steadily diminished when the concentration was further decreased from 0.1 to 0.002 mM without showing any blueshift (inset, Figure 4a). The concentration variation CD plots of **2** in *n*-dodecane were also similar to the behavior of gelator **1**. The 335 nm band at 2.72 mM

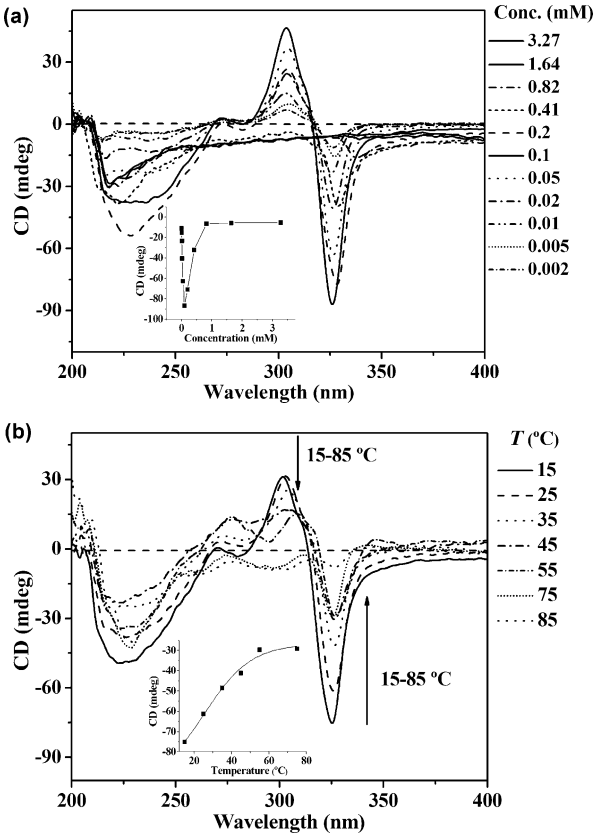

Figure 4. a) Concentration-dependent changes in the CD spectra of **1** in *n*-dodecane at 25 °C; inset shows the plot of CD (in millidegrees (mdeg)) versus concentration at 326 nm. b) Temperature-dependent changes in the CD spectra of **1** in *n*-dodecane at the concentration of 0.03 mM; inset shows the plot of CD (mdeg) versus temperature at 326 nm.

shifted to 320 nm at 0.02 mM. The intensity of the peak near 335 nm increased on decreasing concentration up to 0.34 mM and steadily decreased on further dilution, which is clearly evident from Figure S3a in the Supporting Information. This behavior showed that aggregation was induced by **2** in the *n*-dodecane although it did not form a physical gel. Similarly, concentration-dependent CD spectra **3** and **4** showed a significant decrease in the intensity of 220 nm peak due to the weakening of H-bonding (see Figure S3b and c in the Supporting Information). However, the existence of the negative band at 220 nm indicates that they also adopt β-sheet-type arrangements in the aggregates.

Concentration-dependent CD spectra in *n*-dodecane revealed that all the peaks were not resolved at high concentration (>0.41 mM) due to spectral broadening. Since aggregation is still retained at the lower concentrations, we recorded the temperature-dependent CD spectra of **1** in a dilute solution (0.03 mM), in which each peak was clearly visible.[17a,26b] The variable-temperature CD spectra of **1** showed changes in the intensity of the CD bands upon increasing temperature from 15 to 85 °C (Figure 4b). An interesting phenomenon was observed near 326 nm in which the CD spectra of gelator **1** in *n*-dodecane showed a negative Cotton effect. The negative CD band at 326 nm and positive

signal at 304 nm started to quench with increasing temperature up to 85 °C because of the destruction of supramolecular chirality, which was clearly visible when we plotted the intensity of the CD peak at 326 nm as a function of temperature (Inset, Figure 4b). The negative CD band at 326 nm quenched in a more pronounced fashion compared with the positive band at 304 nm. Additionally, the positive peak at 304 nm at 15 °C shifted to 308 nm at 85 °C. However, the 326 nm band did not shift during the thermotropic transition. The transition temperature (ca. 53 °C) was calculated from the plot of the CD intensity at 326 nm versus temperature for the disruption of the self-assembly to smaller aggregates. Even at 85 °C, the CD signal at 220 nm did not disappear completely, which indicated that even when the molecules were in the sol state, few small aggregates still persisted. This clearly indicates that the supramolecular chirality of the self-assembled aggregates in the gel state is responsible for the observed helicity (see below).[27] Compound **2** in *n*-dodecane, containing two L-phenylalanine moieties in place of L-alanine of **1** showed a similar behavior in the CD spectroscopy upon temperature variation. With increasing temperature, the intensity of the negative peaks at 220, 270, and 320 nm decreased. However, an interesting phenomenon was observed at 65 °C. The CD band intensity at 270 and 320 nm diminished followed by the appearance of two positive bands at 280 and 330 nm possibly due to the secondary structural transformation (see Figure S4a in the Supporting Information).[28] Gelators **3** and **4** contained L-alanine and L-phenylalanine residue only at one branch. Both of these compounds showed a temperature-variable CD spectral pattern unlike compound **1** and **2** (see Figure S4b and c in the Supporting Information). Only a little change was observed at 220 nm during thermotropic transition indicating the existence of strongly bound H-bonded network in the monosubstituted amino acid derivatives.

Morphological features: The superstructures created by the organogel networks were examined under TEM, SEM, and AFM. The freeze-dried gels of **5** revealed the presence of fibrous networks with a fiber width of 1–2 μm (see Figure S5 in the Supporting Information). A comparatively larger aggregated morphology was observed for **1**, **3**, and **4** under SEM because the introduction of an extra amide interaction brings the smaller aggregates close to each other to form aggregates of longer length. The TEM images of gelator **1**, **3**, and **4** in *n*-dodecane showed entangled nanofibers of very high aspect ratio and diameters ranged from 20–30 nm for **1** and 100–500 nm for **3** and **4** (see Figure S6 in the Supporting Information). However, compound **5** exhibited microtapes with diameters ranging from 0.5–1.0 μm.

Figure 5a–d shows the AFM images of dodecane gels of **1**, **3**, **4**, and **5**. The gel of **5** exhibited uniform tapes with diameters ranged from 1–5 μm. However, entangled nanofibers (50–100 nm) were obtained in the *n*-dodecane gel of **4**. Interestingly, gels from **1** and **3** containing di- and monosubstituted L-alanine spacers showed left-handed and right-handed helical nanofibers (50–100 nm), respectively, of high aspect ratio. Parquette and co-workers observed similar results with certain naphthalene diimide (NDI)-appended dipeptides.[29] Such NDI-dipeptides formed amyloid-like helical nanofibers and twisted nanoribbons depending on the placement of the NDI group, in which β-sheet-type hydrogen bonding and π–π association played important roles in directing the assembly process.

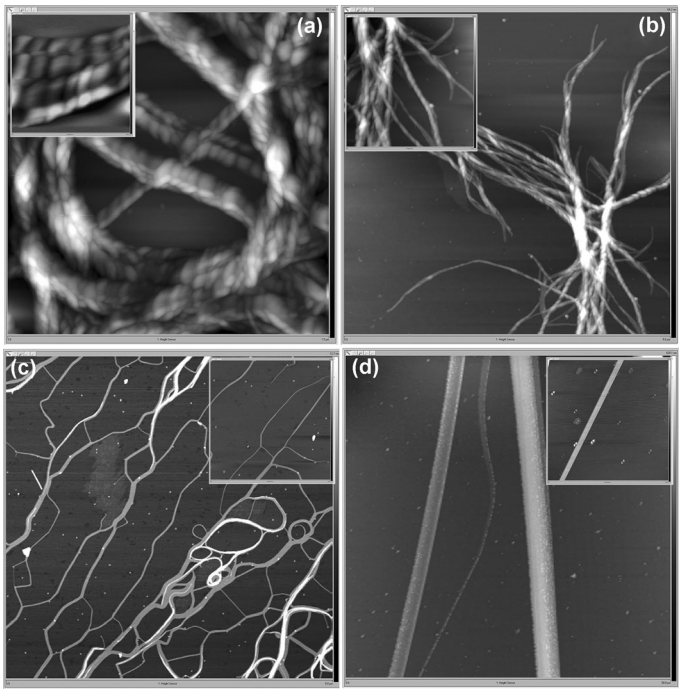

Figure 5. AFM images of the xerogels derived from a) **1**, b) **3**, c) **4**, and d) **5**, respectively, in *n*-dodecane.

FTIR spectroscopy: The presence of extensive H-bonding was also confirmed by concentration-dependent IR spectroscopy. Figure 6 shows the IR-stretching frequencies of the "strong" gel, the "weak" gel, and the "sol" of **3** in dodecane. The N–H stretching frequency at 3280 cm^{-1} in the "strong" gel (2 mM) shifted to 3290 cm^{-1} in the "weak" gel (1 mM) and 3295 cm^{-1} in the "sol" state (0.5 mM). Thus, the stretch-

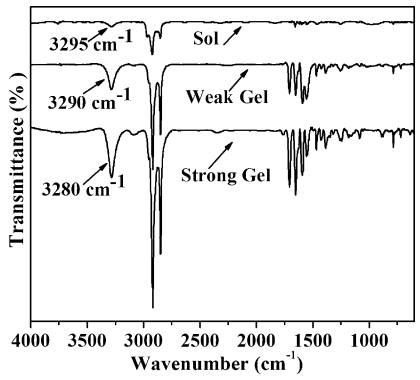

Figure 6. Concentration-dependent changes in the FTIR spectra of **3** in *n*-dodecane.

ing frequency shifted to higher wavenumbers on dilution indicating a progressive decrease of the intermolecular H-bonding by the participation of gelators in the self-assembly.[2c,17a,23] A similar behavior observed in other instances under the concentration variation and the shifts in the stretching frequencies were 26 for **1**, 32 for **4**, and 12 cm^{-1} for **5** (see Figure S7 in the Supporting Information).

Small-angle and wide-angle X-ray diffraction: Small-angle X-ray diffraction (SAXD) was carried out to acquire information about the packing pattern in the supramolecular assembly. The diffraction patterns of each of these xerogels showed three peaks, which were in the ratio of 1:0.5:0.33 indicating a lamellar-type aggregation pattern (Figure 7a). The SAXD pattern of the xerogel of **5** obtained from *n*-dodecane showed three peaks corresponding to the *d* value at 3.66 nm, 1.83 nm, which is in the ratio of 1:0.5, and 1.22 nm (1:0.33), thus indicating a lamellar pattern of the aggregates of gel **5** with an interlayer spacing of 3.66 nm.[30] Similarly the *d* spacing was observed for xerogel of **1** at 3.52 nm, 1.76 nm (1:0.5), 1.15 nm (1:0.33); xerogel of **3** at 3.42 nm, 1.71 nm (1:0.5), 1.14 nm (1:0.33) and xerogel of **4** at 3.54 nm, 1.74 nm (1:0.5), 1.18 nm (1:0.33) indicating the presence of a lamellar structure (see Figure S8 in the Supporting Information). The WAXD profiles showed sharp reflections in the 2θ range of 18–30°, which were typical of a crystalline arrangement of long alkyl side-chains (see Figure S9 in the Supporting Information).[30b]

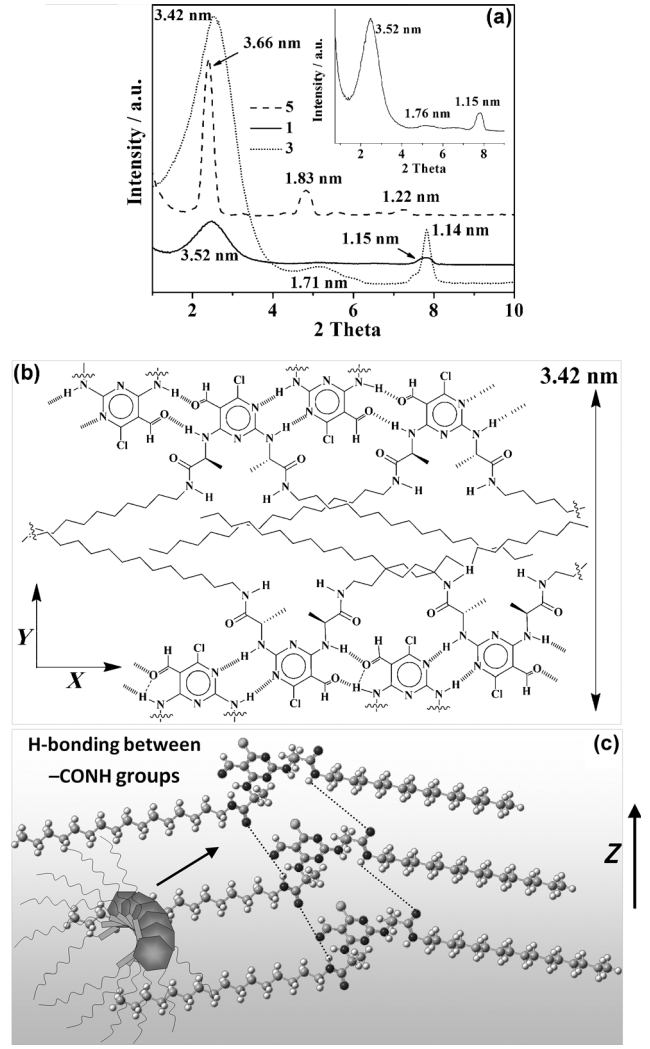

Figure 7. a) Small-angle XRD plot of xerogel of **1**, **3**, and **5** obtained from *n*-dodecane. Inset showing magnification of **1** for clarity. b) Schematic illustration of the lamellar structure of **1** in the *xy* plane through complementary intermolecular hydrogen-bonding. c) Proposed molecular packing of propagation of the aggregates of **1** along the direction (*z* axis) of the growth of supramolecular fibrous networks through interlayer hydrogen-bonding of the −CONH groups.

Energy minimization and the proposed model of self-assembly: Figure S10a in the Supporting Information shows the ground-state geometry of the symmetrical **1** optimized by using B3LYP/6-31G* program in the gas phase. The results indicate that the long aliphatic chains are directed opposite to each other with longest molecular length of 2.7 nm starting from the central aromatic core. The molecular lengths in their optimized geometries are comparable in all the analogous compounds (see Figure S10b–e in the Supporting Information).

SAXD studies of **1** revealed the presence of periodic lamellar structures with repeat distances of 3.52 nm, which is less than the double of the molecular lengths. This indicates that the long alkyl chains in **1** interdigitate with each other through the van der Waals interactions among them.[31] This in turn, brings the pyrimidine rings into close proximity to form extended hydrogen-bonded networks. Pyrimidine derivatives are well-known to form complementary H-bonded structures.[17c,32] The molecules described herein also possess complementary H-bonding functions, which occur through the participation of sp^2-hybridized ring nitrogen atoms, −NH, and aldehyde groups (Figure 7b). These 2D-supramolecular aggregates propagate in the orthogonal direction of the molecular plane through interlayer H-bonding between the −CONH groups (Figure 7c) to form a 3D self-assembly. Such a system is indeed supported from their CD signatures, which are very similar to β-sheet-type structures that are formed in peptides. Based on the results from CD and IR spectroscopies, SAXD analysis and energy minimization calculations we have proposed a packing model of the self-assembly (Figure 7b and c).[29] Interestingly, the optimized structure of **5** shows some differences from the other members. The lack of a methyl/phenyl group near to the pyrimidine ring favors the residues to be in close proximity. This results in a geometry which is much closer to a "V"-shaped conformation. SAXD analysis of **5** confirmed lamellar type of arrangements with a repeat distance of 3.66 nm, which is fairly close to double the molecular lengths calculated from the optimized molecular geometry. This precludes the probability of interdigitation of the hydrophobic chains in **5** perhaps due to the presence of dipole–dipole interactions among the ester groups.

Rheology experiment: Rheological studies of each supramolecular gel confirmed their viscoelastic properties. Since each gelator exhibited a lower mgc in *n*-dodecane compared with that in *n*-heptane, rheological measurements were performed in *n*-dodecane. Oscillatory frequency sweep and amplitude sweep experiments were performed to find out the storage and loss moduli (G′ and G″). In principle, the storage (or elastic) modulus G′ represents a solid-like character, that is, the ability of the material to resist deformation under stress. In contrast the loss (or viscous) modulus G″ reflects the liquid-like behavior, that is, the propensity of the material to flow. Generally, the gels show higher magnitude of G′ values than the G″ values, demonstrating an evidence of the viscoelastic behavior. In an oscillatory amplitude sweep experiment, the crossover point of G′ and G″ is termed as yield stress (σ_y) in which the transition of the elastic solid-like character to the viscous liquid-like character occurs.

The flow behavior of the gel was measured by using a simple rotational flow curve experiment. With increasing shear rate, the viscosity of the *n*-dodecane gel decreased almost linearly indicating that the gels behaved as viscoelastic solid-like and shear-thinning material (see Figure S11 a in the Supporting Information). The frequency sweep experiment of dodecane gels of **5** and **3** demonstrated comparable elastic storage modulus, G′ (ca. 27000 Pa), which was always greater than the associated loss modulus, G“, in the angular frequency range 0.1–500 rad s^{-1} under an initial strain of 0.001 %, thereby indicating the viscoelastic nature of the gel over the entire angular frequency range (see Figure S11 b in the Supporting Information).[2f] The G′ value of gel of **1** was approximately 9000 Pa and it decreased further in the gel derived from **4** (G′≈200 Pa). This result clearly indicates that the presence of the L-phenylalanine-based spacer reduces the viscoelasticity of the present system.

The viscoelastic behavior of the *n*-dodecane gels was found to be similar under the amplitude sweep experiment as with the frequency sweep experiment. There was no significant difference in the G′ of **5** and **3** and the value was approximately 26000 Pa; whereas in **1** (G′≈4000 Pa) and **4** (G′≈600 Pa), the values were significantly less. These data indicate that the viscoelasticity of the gelator is greater when there is no chiral spacer (compound **5**) or when the gelator is functionalized only at one end by one L-alanine residue (compound **3**). However, when the gelator was crafted with L-alanine at both sides (compound **1**), the viscoelasticity decreased further. When L-phenylalanine was inserted at one end of the gelator (compound **4**), there was a decrease in the viscoelasticity probably due to the larger size of the phenyl side-chain, which most probably induced steric crowding to compromise with the compact packing required for the manifestation of higher viscoelasticity.

Each gel has its own characteristic yield stress (σ_y) according to its viscoelasticity to an external oscillating stress (Figure 8). When the *n*-dodecane gels made from **1**, **3**, **4**, and **5** succumbed to the applied stress, only those of **1** and **4** started to flow at a shear stress of 10 Pa and of 1 Pa, respectively. However, compounds **3** and **5** began to lose their solid-like flow behavior only at a shear stress of approximately 100 Pa. These results indicate that the trend in viscoelastic behavior of these gelators is **5**≈**3**>**1**>**4**. The trends in their yield stress values signify that the gelator **3** (containing one L-alanine spacer) and the achiral compound **5** are most resistant to flow under an applied mechanical force. Whereas, gelator **4** (one L-phenylalanine spacer) showed least yield stress value. This may be again attributed to the steric crowding of the side chains as discussed before.

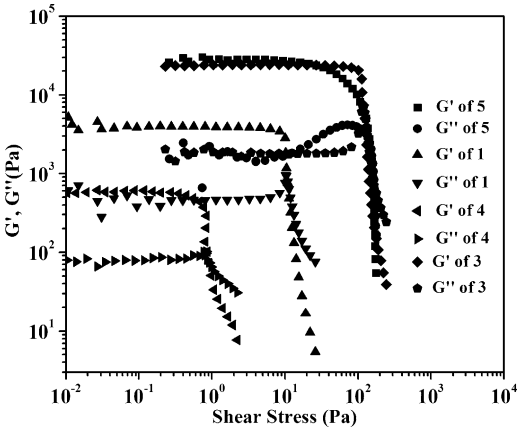

Figure 8. Rheological measurements show oscillatory amplitude sweep experiment of the gels derived from **1**, **3**, **4**, and **5** in *n*-dodecane (concentration = 10 mM in each case).

Differential scanning calorimetry (DSC) and polarized optical microscopy (POM): Solid phase DSC and POM experiments are well-known and useful techniques for the investigation of the thermotropic behavior.[33] The DSC profile of compound **3** showed a small endothermic transition at 85 °C and a larger endothermic peak at 95 °C (Figure 9 a). However, compound **4** showed a large, broad endothermic transition at 116 °C. In the cooling cycle, both of them showed double exothermic transitions at 79 and 53 °C for **3** and 98 and 78 °C for **4**. Larger peaks appeared at higher temperatures and the smaller exothermic transitions appeared at lower temperature during cooling in both the cases. On the other hand, compound **5** showed a single and sharp peak at 80 °C during heating and at 53 °C on the cooling cycle. It has been observed that amino acid-bearing molecules have higher melting temperatures compared with the analogous compound (**5**) without any amino acid moiety. An interesting phenomenon was observed in the DSC profiles of **1** and **2** (see Figure S12 in the Supporting Information). These compounds contained identical amino acid branches on both sides. The kinetics of the crystallization process of such compounds was so slow that they did not show any exothermic peak in the cooling cycle immediately upon melting. Therefore, they were kept at room temperature for 24 h for crystallization. After annealing at room temperature for 24 h, they were allowed to undergo one more heating and cooling cycle. The heating cycle showed broad endothermic transitions and again the cooling cycle did not show any peak.[34]

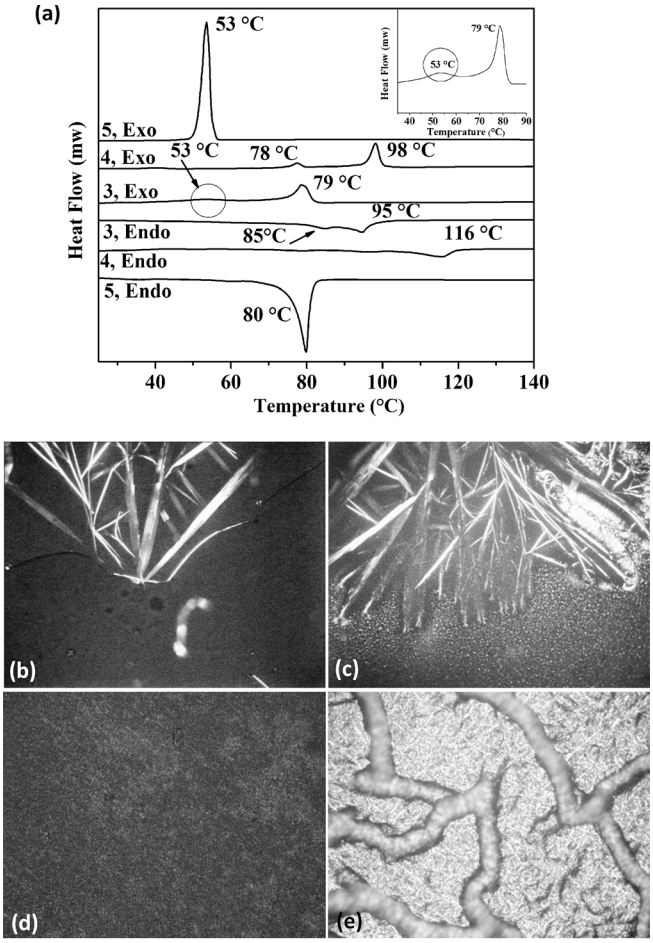

Figure 9. a) Solid phase DSC profiles of **3**, **4** and **5**. Inset shows magnification of the exothermic scan of **3** for clarity. The circled zone appears as a clear peak in the inset. POM images of **3** were captured at b) 80 °C and c) 55 °C. POM images of **4** at d) 100 °C and e) 75 °C. Magnification = 20×.

To illustrate more about the thermotropic behavior, we investigated the samples under a polarized optical microscope. The sample was first heated to get an isotropic melt and then slowly cooled down to room temperature at the same rate of the DSC experiment (5 °C min^{-1}). A thermotropic transition was observed during cooling and different crystalline birefringent textures appeared upon changing temperature. Birefringent phases of **3** started appearing at 80 °C, at which a large crystalline phase was observed that was associated with a large exothermic transition in the DSC profile (Figure 9b). The birefringent texture shifted drastically to a new type of phase with a small crystalline morphology when cooled to 55 °C, corresponding to the small exothermic peak in the DSC curve; the texture was retained upon cooling further to 30 °C (Figure 9c). A similar type of biphasic behavior was also observed under the POM images of **4**, in which the birefringent texture started appearing at 100 °C followed by the appearance of a different type of texture at 75 °C, which are in accordance with the DSC thermotropic profile (Figure 9d and e). This kind of biphasic transition of monosubstituted derivatives (**3** and **4**) is similar to the thermotropic behavior of 4-chloro-2,6-bis(octadecylamino)pyrimidine-5-carbaldehyde reported by Fenniri et al.[17c] However, compound **5** did not show any biphasic behavior, which supported the single peak appeared at 53 °C in the DSC experiment (see Figure S13 in the Supporting Information). Interesting observations were noted in the POM experiment of **1** and **2** (see Figure S13 in the Supporting Information). Each of these compounds contained two identical L-amino acid branches. No crystalline phase appeared immediately during the cooling of the isotropic melt. However, small crystals started appearing after the sample remained at room temperature for 24 h. These phenomena also explain the absence of peak in their cooling curve of their DSC profiles. The presence of an L-alanine or L-phenylalanine substituent on both the sides of the di-substituted derivatives (**1** and **2**) presumably drives the aliphatic chains apart from each other, which probably impedes the compact packing of the molecules leading to the slow crystallization of the isotropic melt.

Conclusion

In this work, we have described the syntheses and properties upon the self-assembly exhibited by a new family of 2,4,6-trichloropyrimidine-5-carbaldehyde derivatives tailored with number of H-bonding motifs depending on the nature and number of chirally pure amino acid moieties inserted as a spacer. The role of amino acid moieties on their self-assembly leading to the formation of β-sheet type structure of the chiral supramolecular aggregates was explored by using UV/Vis and CD spectroscopies. Generally, the β-sheet type arrangement is quite regular in the self-assemblies of the peptides in aqueous solution. However, here we show a rare manifestation in which the extensively H-bonded self-assembly of small organic molecule in aliphatic hydrocarbons mimics the β-sheet type organization. The effect of H-bonding on the self-assembly by temperature and concentration variation was also demonstrated by using UV/Vis and CD spectroscopies. Due to the presence of extra pair of H-bonding donor and acceptor sites of the amide linkages of the amino acids, the extent of H-bonding increased as probed by using FTIR studies. This complementary H-bonding led them to exist as periodic lamellar structure, which was confirmed by a SAXD study.

Interestingly, gelator **1** and **3** containing di- and monosubstituted L-alanine residues exhibited helical nanofibers of high aspect ratio as discerned from AFM studies. Thus, incorporation of L-alanine has been found to be useful to exaggerate the chiral signature from the molecular to the microscopic level. However, incorporation of L-phenylalanine as spacer produced only simple nanofibers. This shows the importance of subtle balance in packing imposed by the side chains of the L-amino acid spacers. Depending on the amino acid moiety these molecules exhibited interesting thermotropic behavior, which is reflected in the POM and DSC studies. Hence, this work sheds a new light in the self-assem-

bly phenomenon, in which the properties of the chiral supramolecular assembly could be modulated by fine-tuning of their molecular features.

Acknowledgements

This work was supported by the Department of Science and Technology (J. C. Bose Fellowship to S.B.), and the Government of India, New Delhi, India. S.D. thanks CSIR for a senior research fellowship.

[1] a) G. Tikhomirov, T. Yamazaki, A. Kovalenko, H. Fenniri, *Langmuir* **2008**, *24*, 4447–4450; b) G. M. Whitesides, B. Grzybowski, *Science* **2002**, *295*, 2418–2421; c) H. Fenniri, P. Mathivanan, K. L. Vidale, D. M. Sherman, K. Hallenga, K. V. Wood, J. G. Stowell, *J. Am. Chem. Soc.* **2001**, *123*, 3854–3855.

[2] a) S. Bhattacharya, S. K. Samanta, *Langmuir* **2009**, *25*, 8378–8381; b) S. K. Samanta, A. Pal, S. Bhattacharya, *Langmuir* **2009**, *25*, 8567–8578; c) M. George, R. G. Weiss, *Acc. Chem. Res.* **2006**, *39*, 489–497; d) G. Mieden-Gundert, L. Klein, M. Fischer, F. Vögtle, K. Heuzé, J.-L. Pozzo, M. Vallier, F. Fages, *Angew. Chem.* **2001**, *113*, 3266–3267; *Angew. Chem. Int. Ed.* **2001**, *40*, 3164–3166; e) P. Terech, R. G. Weiss, *Chem. Rev.* **1997**, *97*, 3133–3160; f) S. Bhattacharya, S. N. G. Acharya, A. R. Raju, *Chem. Commun.* **1996**, 2101–2102.

[3] a) S. K. Samanta, K. S. Subrahmanyam, S. Bhattacharya, C. N. R. Rao, *Chem. Eur. J.* **2012**, *18*, 2890–2901; b) H. Basit, A. Pal, S. Sen, S. Bhattacharya, *Chem. Eur. J.* **2008**, *14*, 6534–6545; c) S. Bhattacharya, A. Srivastava, A. Pal, *Angew. Chem.* **2006**, *118*, 3000–3003; *Angew. Chem. Int. Ed.* **2006**, *45*, 2934–2937.

[4] a) G. A. Silva, C. Czeisler, K. L. Niece, E. Beniash, D. A. Harrington, J. A. Kessler, S. I. Stupp, *Science* **2004**, *303*, 1352–1355; b) J. D. Hartgerink, E. Beniash, S. I. Stupp, *Science* **2001**, *294*, 1684–1688.

[5] a) H. Yang, T. Yi, Z. Zhou, Y. Zhou, J. Wu, M. Xu, F. Li, C. Huang, *Langmuir* **2007**, *23*, 8224–8230; b) Z. Dzolic, M. Cametti, A. D. Cort, L. Mandolini, M. Zinic, *Chem. Commun.* **2007**, 3535–3537; c) C. Wang, D. Zhang, D. Zhu, *Langmuir* **2007**, *23*, 1478–1482; d) J. E. A. Webb, M. J. Crossley, P. Turner, P. Thordarson, *J. Am. Chem. Soc.* **2007**, *129*, 7155–7162; e) H. Maeda, Y. Haketa, T. Nakanishi, *J. Am. Chem. Soc.* **2007**, *129*, 13661–13674; f) P. Mukhopadhyay, Y. Iwashita, M. Shirakawa, S.-i. Kawano, N. Fujita, S. Shinkai, *Angew. Chem.* **2006**, *118*, 1622–1625; *Angew. Chem. Int. Ed.* **2006**, *45*, 1592–1595; g) A. Ghoussoub, J. M. Lehn, *Chem. Commun.* **2005**, 5763–5765.

[6] a) S. Matsumoto, S. Yamaguchi, S. Ueno, H. Komatsu, M. Ikeda, K. Ishizuka, Y. Iko, K. V. Tabata, H. Aoki, S. Ito, H. Noji, I. Hamachi, *Chem. Eur. J.* **2008**, *14*, 3977–3986; b) Q. Liu, Y. Wang, W. Li, L. Wu, *Langmuir* **2007**, *23*, 8217–8223; c) C. Shi, J. Zhu, *J. Chem. Mater.* **2007**, *19*, 2392–2394; d) W. Weng, J. B. Beck, A. J. Jamieson, S. J. Rowan, *J. Am. Chem. Soc.* **2006**, *128*, 11663–11672.

[7] a) S. Bhattacharya, S. K. Samanta, *Chem. Eur. J.* **2012**, *18*, 16632–16641; b) S. K. Samanta, S. Bhattacharya, *J. Mater. Chem.* **2012**, *22*, 25277–25287; c) M. Shirakawa, N. Fujita, T. Tani, K. Kaneko, M. Ojima, A. Fujii, M. Ozaki, S. Shinkai, *Chem. Eur. J.* **2007**, *13*, 4155–4162; d) S. Wang, W. Shen, Y. Feng, H. Tian, *Chem. Commun.* **2006**, 1497–1499; e) M. Carrasco-Orozco, W. C. Tsoi, M. O'Neill, M. P. Aldred, P. Vlachos, S. M. Kelly, *Adv. Mater.* **2006**, *18*, 1754–1758; f) M. O'Neill, S. M. Kelly, *Adv. Mater.* **2003**, *15*, 1135–1146; g) L. Schmidt-Mende, A. Fechtenkotter, K. Müllen, E. Moons, R. H. Friend, J. D. MacKenzie, *Science* **2001**, *293*, 1119–1122.

[8] a) T. Tu, W. Assenmacher, H. Peterlik, R. Weisbarth, M. Nieger, K. H. Dötz, *Angew. Chem.* **2007**, *119*, 6486–6490; *Angew. Chem. Int. Ed.* **2007**, *46*, 6368–6371; b) J. F. Miravet, B. Escuder, *Chem. Commun.* **2005**, 5796–5798.

[9] a) M. George, S. L. Synder, P. Terech, C. J. Glinka, R. G. Weiss, *J. Am. Chem. Soc.* **2003**, *125*, 10275–10283; b) T. Kato, T. Kutsuna, K. Hanabusa, M. Ukon, *Adv. Mater.* **1998**, *10*, 606–608; c) K. Hanabusa, M. Yamada, M. Kimura, H. Shirai, *Angew. Chem.* **1996**, *108*, 2086–2088; *Angew. Chem. Int. Ed. Engl.* **1996**, *35*, 1949–1951.

[10] a) S. Bhattacharya, S. N. G. Acharya, *Chem. Mater.* **1999**, *11*, 3121–3132; b) K. Hanabusa, K. Okui, K. Karaki, M. Kimura, H. Shirai, *J. Colloid Interface Sci.* **1997**, *195*, 86–93.

[11] a) G. Wang, A. D. Hamilton, *Chem. Commun.* **2003**, 310–311; b) F. S. Schoonbeek, J. H. van Esch, B. Wegewijs, D. B. A. Rep, M. P. de Haas, T. M. Klapwijk, R. M. Kellogg, B. L. Feringa, *Angew. Chem.* **1999**, *111*, 1486–1490; *Angew. Chem. Int. Ed.* **1999**, *38*, 1393–1397.

[12] a) G. John, G. Zhu, J. Li, J. S. Dordick, *Angew. Chem.* **2006**, *118*, 4890–4893; *Angew. Chem. Int. Ed.* **2006**, *45*, 4772–4775; b) J. H. Jung, S. Shinkai, T. Shimizu, *Chem. Eur. J.* **2002**, *8*, 2684–2690; c) J. H. Jung, G. John, M. Masuda, K. Yoshida, S. Shinkai, T. Shimizu, *Langmuir* **2001**, *17*, 7229–7232; d) K. Yoza, N. Amanokura, Y. Ono, T. Akao, H. Shinmori, M. Takeuchi, S. Shinkai, D. N. Reinhoudt, *Chem. Eur. J.* **1999**, *5*, 2722–2729; e) S. Bhattacharya, S. N. G. Acharya, *Chem. Mater.* **1999**, *11*, 3504–3511.

[13] a) L. Lu, T. M. Cocker, R. E. Bachman, R. G. Weiss, *Langmuir* **2000**, *16*, 20–34; b) C. Geiger, M. Stanescu, L. H. Chen, D. G. Whitten, *Langmuir* **1999**, *15*, 2241–2245; c) R. Mukkamala, R. G. Weiss, *Langmuir* **1996**, *12*, 1474–1482; d) K. Murata, M. Aoki, T. Suzuki, T. Harada, H. Kawabata, T. Komori, F. Ohseto, K. Ueda, S. Shinkai, *J. Am. Chem. Soc.* **1994**, *116*, 6664–6676.

[14] a) S. Kawano, N. Fujita, K. J. C. van Bommel, S. Shinkai, *Chem. Lett.* **2003**, *32*, 12–13; b) M. Suzuki, M. Yumoto, M. Kimura, H. Shirai, K. Hanabusa, *Chem. Eur. J.* **2003**, *9*, 348–354; c) T. Ishi-i, R. Iguchi, E. Snip, M. Ikeda, S. Shinkai, *Langmuir* **2001**, *17*, 5825–5833.

[15] a) H. Dai, Q. Chen, H. Qin, Y. Guan, D. Shen, Y. Hua, Y. Tang, J. Xu, *Macromolecules* **2006**, *39*, 6584–6589; b) A. Motulsky, M. Lafleur, A.-C. Couffin-Hoarau, D. Hoarau, F. Boury, J.-P. Benoit, J.-C. Leroux, *Biomaterials* **2005**, *26*, 6242–6253.

[16] a) X. Tong, Y. Zhao, B.-K. An, S. Y. Park, *Adv. Funct. Mater.* **2006**, *16*, 1799–1804; b) A. Kishimura, T. Yamashita, T. Aida, *J. Am. Chem. Soc.* **2005**, *127*, 179–183; c) O. Roubeau, A. Colin, V. Schmitt, R. Clérac, *Angew. Chem.* **2004**, *116*, 3345–3348; *Angew. Chem. Int. Ed.* **2004**, *43*, 3283–3286.

[17] a) S. Datta, S. Bhattacharya, *Chem. Commun.* **2012**, *48*, 877–879; b) P. Sahoo, R. Sankolli, H.-Y. Lee, S. R. Raghavan, P. Dastidar, *Chem. Eur. J.* **2012**, *18*, 8057–8063; c) C. Danumah, R. L. Beingessner, A. Haque, F. Ban, J. P. Richards, A. Kovalenko, H. Fenniri, *Langmuir* **2009**, *25*, 11857–11861; d) K. J. C. van Bommel, C. van der Pol, I. Muizebelt, A. Friggeri, A. Heeres, A. Meetsma, B. L. Feringa, J. van Esch, *Angew. Chem.* **2004**, *116*, 1695–1699; *Angew. Chem. Int. Ed.* **2004**, *43*, 1663–1667; e) K. J. C. van Bommel, A. Friggeri, S. Shinkai, *Angew. Chem.* **2003**, *115*, 1010–1030; *Angew. Chem. Int. Ed.* **2003**, *42*, 980–999; f) T. Kato, *Science* **2002**, *295*, 2414–2418; g) W. Kubo, T. Kitamura, K. Hanabusa, Y. Wada, S. Yanagida, *Chem. Commun.* **2002**, 374–375; h) D. J. Abdallah, R. G. Weiss, *Adv. Mater.* **2000**, *12*, 1237–1247.

[18] a) H. Yang, H. Liu, H. Kang, W. Tan, *J. Am. Chem. Soc.* **2008**, *130*, 6320–6321; b) D. J. Pochan, J. P. Schneider, J. Kretsinger, B. Ozbas, K. Rajagopal, L. Haines, *J. Am. Chem. Soc.* **2003**, *125*, 11802–11803; c) J. P. Schneider, D. J. Pochan, B. Ozbas, K. Rajagopal, L. Pakstis, J. Kretsinger, *J. Am. Chem. Soc.* **2002**, *124*, 15030–15037.

[19] S. Bhattacharya, Y. Krishnan-Ghosh, *Chem. Commun.* **2001**, 185–186.

[20] a) A. Prathap, K. M. Sureshan, *Chem. Commun.* **2012**, *48*, 5250–5252; b) A. C. Couffin-Hoarau, A. Motulsky, P. Delmas, J. C. Leroux, *J. Pharm. Res. Dev.* **2004**, *21*, 454–457; c) D. R. Trivedi, A. Ballabh, P. Dastidar, B. Ganguly, *Chem. Eur. J.* **2004**, *10*, 5311–5322.

[21] a) G. John, S. R. Jadhav, V. M. Menon, V. T. John, *Angew. Chem. Int. Ed.* **2012**, *51*, 1760–1762; b) S. R. Jadhav, P. K. Vemula, R. Kumar, S. R. Raghavan, G. John, *Angew. Chem.* **2010**, *122*, 7861–7864; *Angew. Chem. Int. Ed.* **2010**, *49*, 7695–7698.

[22] a) M. J. I. Andrews, A. B. Tabor, *Tetrahedron* **1999**, *55*, 11711–11743; b) C. L. Nesloney, J. W. Kelly, *Bioorg. Med. Chem.* **1996**, *4*, 739–766.

[23] S. Bhattacharya, A. Pal, *J. Phys. Chem. B* **2008**, *112*, 4918–4927.
[24] R. L. Beingessner, B. L. Deng, P. E. Fanwick, H. Fenniri, *J. Org. Chem.* **2008**, *73*, 931–939.
[25] A. Barbatu, I.-C. Stancu, R.-A. Mitran, S. Tomas, *U. P. B. Sci. Bull., Series B* **2011**, *73*, 135–142.
[26] a) M. Ma, Y. Kuang, Y. Gao, Y. Zhang, P. Gao, B. Xu, *J. Am. Chem. Soc.* **2010**, *132*, 2719–2728; b) A. Shome, S. Debnath, P. K. Das, *Langmuir* **2008**, *24*, 4280–4288; c) L. A. Haines, K. Rajagopal, B. Ozbas, D. A. Salick, D. J. Pochan, J. P. Schneider, *J. Am. Chem. Soc.* **2005**, *127*, 17025–17029; d) P. K. Sarkar, P. Doty, *Proc. Natl. Acad. Sci. USA* **1966**, *55*, 981–989; e) R. Townend, T. F. Kumosinski, S. N. Timasheff, G. D. Fasman, B. Davidson, *Biochem. Biophys. Res. Commun.* **1966**, *23*, 163–169; f) C. Toniolo, G. M. Bonora, S. Salardi, M. Mutter, *Macromolecules* **1979**, *12*, 620–625; g) S. Brahms, J. Brahms, G. Spach, A. Brack, *Proc. Natl. Acad. Sci. USA* **1977**, *74*, 3208–3212; h) E. Iizuka, J. T. Yang, *Proc. Natl. Acad. Sci. USA* **1966**, *55*, 1175–1182.
[27] a) A. Friggeri, C. van der Pol, K. J. C. van Bommel, A. Heeres, M. C. A. Stuart, B. L. Feringa, J. van Esch, *Chem. Eur. J.* **2005**, *11*, 5353–5361; b) A. R. Hirst, D. K. Smith, M. C. Feiters, H. P. M. Geurts, *Chem. Eur. J.* **2004**, *10*, 5901–5910.
[28] J. Cui, A. Liu, Y. Guan, J. Zheng, Z. Shen, X. Wan, *Langmuir* **2010**, *26*, 3615–3622.
[29] H. Shao, T. Nguyen, N. C. Romano, D. A. Modarelli, J. R. Parquette, *J. Am. Chem. Soc.* **2009**, *131*, 16374–16376.
[30] a) J. Kadam, C. F. J. Faul, U. Scherf, *Chem. Mater.* **2004**, *16*, 3867–3871; b) D. J. Abdallah, S. A. Sirchio, R. G. Weiss, *Langmuir* **2000**, *16*, 7558–7561; c) M. Caffrey, J. Hogan, A. S. Rudolph, *Biochemistry* **1991**, *30*, 2134–2146.
[31] a) Y. Chen, Y. Lv, Y. Han, B. Zhu, F. Zhang, Z. Bo, C. Y. Liu, *Langmuir* **2009**, *25*, 8548–8555; b) X. Yang, R. Lu, H. Zhou, P. Xue, P. Wang, P. Chen, Y. Zhao, *J. Colloid Interface Sci.* **2009**, *339*, 527–532.
[32] a) F. H. Beijer, H. Kooijman, A. L. Spek, R. P. Sijbesma, E. W. Meijer, *Angew. Chem.* **1998**, *110*, 79–82; *Angew. Chem. Int. Ed.* **1998**, *37*, 75–78; b) F. H. Beijer, R. P. Sijbesma, H. Kooijman, A. L. Spek, E. W. Meijer, *J. Am. Chem. Soc.* **1998**, *120*, 6761–6769; c) R. P. Sijbesma, F. H. Beijer, L. Brunsveld, B. J. B. Folmer, J. H. K. K. Hirschberg, R. F. M. Lange, J. K. L. Lowe, E. W. Meijer, *Science* **1997**, *278*, 1601–1604.
[33] a) N. Gimeno, J. Barberá, J. L. Serrano, M. B. Ros, *Chem. Mater.* **2009**, *21*, 4620–4630; b) C. W. Yang, T. H. Hsia, C. C. Chen, C. K. Lai, R. S. Liu, *Org. Lett.* **2008**, *10*, 4069–4072; c) N. Steinke, W. Frey, A. Baro, S. Laschat, C. Drees, M. Nimtz, C. Hägele, F. Giesselmann, *Chem. Eur. J.* **2006**, *12*, 1026–1035.
[34] L. Y. Park, J. M. Rowe, *Chem. Mater.* **1998**, *10*, 1069–1075.

Received: February 16, 2013
Published online: June 28, 2013

